Aquatic Toxicology 281 (2025) 107293

Contents lists available at ScienceDirect

Aquatic Toxicology

journal homepage: www.elsevier.com/locate/aqtox

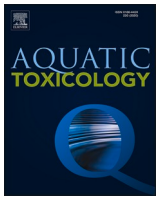

Polar cod early life stage exposure to potential oil spills in the Arctic

Frode B. Vikebø [a,*], Raymond Nepstad [b], Mateusz Matuszak [c], Edel S.U. Rikardsen [c,f], Benjamin J. Laurel [d], Sonnich Meier [a], Elena Eriksen [a], Johannes Röhrs [c], Kai H. Christensen [c,f], Malgorzata Smieszek-Rice [e], Alf Håkon Hoel [f], Mats Huserbråten [a]

[a] Institute of Marine Research, PO Box 1870 Nordnes, 5817, Bergen, Norway
[b] SINTEF Ocean AS, Postboks 4762, NO-7465, Trondheim, Norway
[c] Norwegian Meteorological Institute, Henrik Mohns Plass 1, 0371, Oslo, Norway
[d] Alaska Fisheries Science Center, National Oceanic and Atmospheric Administration, Newport, OR, USA
[e] The Arctic University of Tromsø, Norway
[f] University of Oslo, Oslo, Norway

ARTICLE INFO

Keywords:
Modelling
Oil spill scenarios
Ice edge
Calanus glacialis
Barents Sea
Polar front
Climate change

ABSTRACT

Arctic amplification of climate change is causing sea ice to retreat at unprecedented rates, potentially opening up large vulnerable Arctic areas for oil and gas exploration and new shipping routes. This rapid warming marginalizes sympagic species habitats making them more sensitive to other anthropogenic pressures. Here, we assess potential impacts of hypothetic oil spills from the northernmost licensed oil field Wisting and additional neighbouring spill sites in areas currently not open to oil exploitation on the key ice-associated Arctic fish species polar cod (*Boreogadus saida*). We do this by developing and running combined data-driven models for the ocean, oil spill dispersal and fate, and the early life stages of polar cod. Sea ice and the Polar Front act as natural barriers limiting the exchange of polar cod eggs and larvae and oil spill between Atlantic and Polar Water. However, both barriers vary seasonally so that the sea ice retreats and the Polar Front weakens towards summer causing significant increases in oil exposure to early life stages of polar cod under varying oil spill scenarios investigated here. Previous literature emphasizes that fall feeding conditions must be sufficient for juvenile polar cod to allocate lipids and survive their first winter. Here, we show that less than half the exposed individuals experience these suitable feeding conditions in the fall. The seasonal exposure intensity suggests a need for petroleum regulations with temporal and spatial limitations varying through the year. However, even with these seasonal dynamic regulations in place, climate change induced by the use of fossil fuel will likely reduce these natural barriers through continued sea ice retreat and a weakening of the Polar Front thereby reducing their barrier effects. Risk assessments of anthropogenic impacts on key Arctic ecosystem components in the vicinity of the ice edge zone and the Polar Front will therefore have to be updated to account for these major changes.

1. Introduction

Retreating Arctic sea ice (Skagseth et al., 2020) can open up new areas for oil and gas activity and shipping routes (Melia et al., 2016). As such, oil and gas exploration and exploitation are increasingly considered in high latitudes in the proximity of the ice edge zone. One example includes the Wisting field, located about 300 km north of the mainland Norway and 185 km southeast of the Bear Island and within 50 km of the southernmost extension of ice. If realised, the Wisting project will be the northernmost oil field in the world. New Arctic shipping routes are also increasingly considered with the intrinsic risk of oil spills. Impact assessments therefore need to include oil spill scenarios with oil in ice (Nordam et al., 2020) and dispersal across frontal areas separating cold and fresh Polar Water (PW) with the adjacent warmer and more saline Atlantic Water (AW). Low temperatures may also slow down natural biodegradation of oil (Ferguson et al., 2017) and cause enduring exposure of vulnerable marine species when overlapping. The complexity of oil spill risk assessments also increases dramatically when considering the diversity of ice conditions (e.g. ice thickness, concentration, leads, and drift) and the low empirical knowledge basis of related processes (Nordam et al., 2020).

Sea ice is a key part of Arctic ecosystem structure and functioning

* Corresponding author.
E-mail address: frovik@hi.no (F.B. Vikebø).

https://doi.org/10.1016/j.aquatox.2025.107293
Received 8 October 2024; Received in revised form 17 February 2025; Accepted 17 February 2025
Available online 18 February 2025

(Haug et al., 2017). Seasonal expansion and contraction of the sea ice shape arctic ecosystem phenology by stratifying the water column and affecting solar irradiance penetration through the water column. Ice retreat leaves a blanket of plankton productivity that triggers a rapid spring bloom that cascades into upper trophic levels. The polar cod (*Boerogadus saida*) is a circumpolar mid-trophic Arctic fish species (ACIA, 2005) that links plankton and top predators (Gjøsæter et al., 2020; Eriksen et al., 2020). Polar cod have early life stages (ELS) that are particularly vulnerable to oil spill exposure (Bender et al., 2021; Laurel et al., 2019; Nahrgang et al., 2016). The literature indicates that the threshold for impacts of oil in the water is around 1 μg per liter total polycyclic aromatic hydrocarbons (μg/L TPAH; Laurel et al., 2019) - though the experimental work accounts for dissolved oil only.

The main spawning grounds for polar cod are historically in the southeastern Barents Sea, although retreating sea ice in recent years have shifted spawning grounds into the northwestern Barents Sea (Huserbråten et al., 2019), which became the main spawning area in 2023. Field observations of polar cod are relatively scarce, but fall distributions of the juveniles (age 0, here called 0-group) are collected annually (Eriksen et al., 2020) and can serve as an 'anchorpoint' in connectivity studies. That is, backtracking numerical individual-based models (IBMs) from 0-group polar cod observations may reveal spawning distributions through assumptions on ice conditions, temperature-dependent vital rates, and prey and predator abundance. Using such an approach, Huserbråten et al. (2019) indicated a northward retreat of polar cod spawning grounds towards the northwestern Barents Sea and away from the western Barents Sea Polar Front (PF). These spatial shifts can lead to novel stressors, (e.g. prey limitations, predators and temperature) that can alter survival trajectories of these vulnerable life stages. For example, Copeman et al. (2017) showed that lipid accumulation prior to overwintering is a key to surviving poor feeding conditions. The primary prey items during ELS are the lipid-rich *Calanus glacialis* occupying the northern Barents Sea (Søreide et al., 2010; Bouchard et al., 2016).

The Barents Sea sees the most vessel traffic in the entire Arctic (AMSA, 2009; WGIBAR, 2021), which is largely the result of marine transportation, fisheries and tourism. Although marine traffic is relatively low compared to more southern regions, transportation of oil and gas is common and mainly related to activities in Russian Arctic and along the Norwegian coast. The southern Barents Sea was opened for petroleum activity in 1980 while the northern Barents Sea remains closed, and developments have been generally slow with only 2 of the total 92 identified fields open in Norway. The two active fields in Norwegian waters are Snøhvit and Goliat located in the southwestern Barents Sea. A third field (Johan Castberg) is expected to come on-stream in 2025. Farther north and closer to sea ice, a decision will be made in 2026 whether to develop the Wisting field. If the project goes ahead, production could start some time in the 2030s.

Any oil spill dispersal from spill locations in the Barents Sea will be guided by prevailing winds and ocean currents, with the latter controlled by numerous factors including bottom topography, frontal structures and baroclinic instabilities. Specifically, temperature and salinity delimited AW (>2 °C and >34.8) meet PW (<0 °C and <34.4) in the northwestern Barents Sea giving rise to the PF being topographically locked along the southern flank of the Spitsbergen Bank, across the sill separating the Hopen Trench and the Olga Basin, and continuing south of the Great Bank (Kolås et al., 2024; Lien et al., 2017) (Fig. 2). The position of the PF is more stable in the northwest than in the northeastern Barents Sea. The AW subducts under the PW at depth across the sill while horizontal transport in shallow water is highly seasonal dependent. Kolås et al. (2024) reports of a 50 m surface layer lying above the PF in fall, in contrast to winter conditions when the PF surfaces. Hence, near-surface tracer transport is more decoupled from the PF during fall than during winter, and is therefore less of a barrier for dispersal from AW into PW. Mesoscale eddies enable water mass exchange across the PF from both sides as observed in situ (Kolås et al., 2024) and from remote sensing (Porter et al., 2020), though this exchange is likely underestimated in long-term satellites estimates due to thermal capping (Atadzhanova et al., 2018). However, in general, water mixing across the PF is generally more restricted than mixing within similar type water masses.

In this study, we combine high-resolution ocean model (Regional Ocean Modelling System; ROMS; www.roms.org) archives of the Barents Sea and adjacent seas with an oil and fate dispersal model (OSCAR, Reed et al., 1999) and a polar cod IBM covering egg and larvae stages to assess exposure rates of polar cod ELS for relevant oil spill scenarios. We investigate i) what part of the annual production of polar cod ELS that experiences ambient environmental conditions beneficial for growth and survival, ii) the degree to which the same part of the ELS to a high degree overlaps northern Barents Sea oil spill scenarios, and iii) what oceanographic mechanisms would act as natural barriers or promoters of overlap between polar cod ELS and northern Barents Sea oil spill.

2. Data and methods

2.1. Regional ocean models

Two ocean model applications of ROMS provide the primary data used for forcing the subsequent models (OSCAR, IBM) and for further oceanic analyses. The SVIM archive (Lien et al., 2014) is a 4 × 4 km horizontally resolved ROMS simulation covering the Nordic Seas for the period 1958 until today, which provides daily means of 3D ocean currents, temperature, salinity, turbulence and sea ice. The Barents-2.5 km ROMS simulation (Röhrs et al., 2023) covers the Barents Sea and ocean areas around Svalbard on a 2.5 × 2.5 km horizontal grid, producing hourly means of similar variables as SVIM but for years since 2021.

2.2. Lagrangian coherent structures

Lagrangian Coherent Structures (LCS) in this context are pronounced enduring drift trajectories that are guided by phenomena with a relatively long life span such as steep seabed slopes or oceanic fronts. In order to assess how the PF possibly limits exchange of polar cod ELS and oil spill dispersal between PW and AW we assess the finite time Lyapunov exponents (FTLE), which is an approximation to LCS that is capable of highlighting material accumulation or spreading affiliated with the PF areas. To do this, we initiate particles daily in every grid cell in a subset of the 2021 Barents-2.5 km model domain covering the northern Barents Sea and model repeatedly 24 h intervals throughout the year of dispersal at the fixed depths of both 10 and 100 m based on the hourly modelled currents (Matuszak et al., 2024). The FTLE, here computed forward-in-time, provides a measure of the stretching a fluid parcel experiences over a finite time, and reveals repelling regions in the flow. Elongated features of local FTLE maxima, hereafter called FTLE ridges, may reveal repelling LCSs which are here interpreted as transport barriers for horizontal dispersal. The FTLEs are calculated according to the separation rate between neighbouring particles (see details of the method in Matuszak et al., 2024). In order to investigate seasonality and spatial differences, we calculate FTLEs averaged across the individual months for the entire year of 2021 with a full spatial resolution according to the Barents-2.5 km model grid. Furthermore, we investigate seasonality of the LCSs appearing as expected along the topography supporting the PF using extracted monthly maximum FTLE values at the section shown in Fig. 1.

2.3. Polar cod individual-based model for early life stages

The polar cod ELS IBM is based on the IBM described in Huserbråten et al. (2019). More than 4 million particles are initiated every year in the period 2013–2020 at ocean grid points from the SVIM 4 × 4 km simulation in the Barents Sea shelf shallower than 400 m and with an ice cover of at least 15 % during the period from December 1 to March 31.

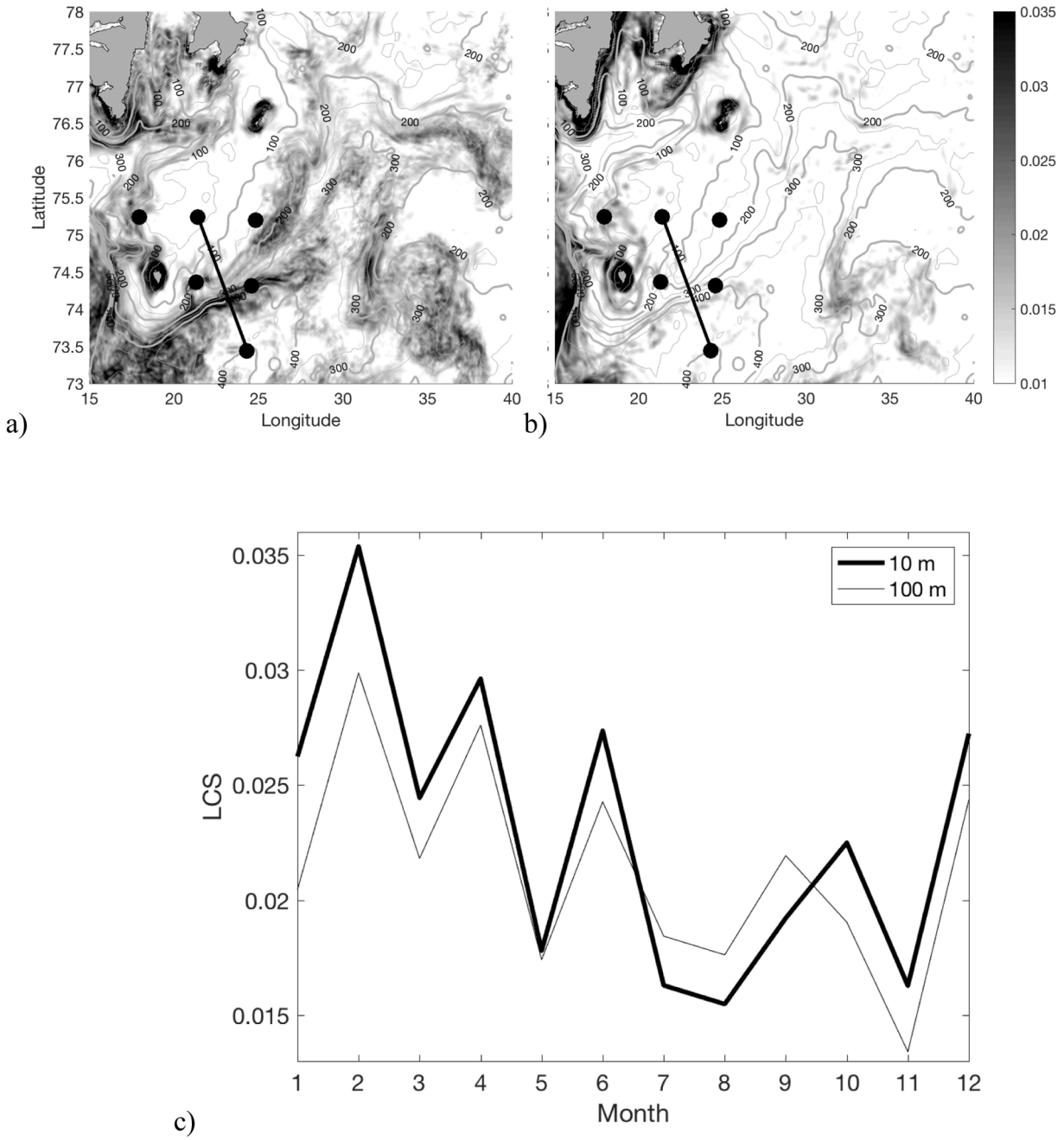

Fig. 1. Average finite time Lyapunov exponent (FTLE, hours^{-1}) for the month of February (a) and July (b) at 10 m depth based on the Barents-2.5 km modelled ocean currents for the year 2021. Maximum monthly mean FTLE across the section indicated in panels a and b between spill site 1 and 5 for the depths 10 and 100 m (c). Spill sites 1–6 are also indicated in panel a and b.

However, only particles initiated below ice (according to SVIM ice module) are considered viable and used in the further processing of the model output. Particles are dispersed using the Runge Kutta 4th order advection scheme and the modelled SVIM currents at depths according to their individual development through egg, larva and juvenile stages. The polar cod IBM egg incubation time was directly related to the modelled temperature field (Laurel et al., 2018), and eggs and pre-feeding larvae were modelled to be vertically positioned as a function of egg/larvae sinking velocities, egg/larvae size (Spencer et al., 2020), and viscosity and density of seawater according to Stokes law at low Reynolds numbers. The growth of the larvae was also temperature dependent from hatching of eggs (at 7 mm) to metamorphosis into the juvenile, extracted from (Vestfals et al., 2021). Vertical position of the larval stages was largely determined by the turbulent mixing field but with larvae swimming upwards or downwards at 0.3 body lengths per second dependent on being below or above the 1 W per m^2 isolume. The buoyant properties of the egg and pre-feeding stages led to a strong surface maxima over most of the year, with the lower tail of the distribution rarely breaking the pycnocline until pelagic juvenile stages (>25 mm) when swimming capabilities enabled individuals to overcome the turbulence field. Swimming below the pycnocline to attain their hypothesized desired depth in relation to the isolume (up to 30 m midday in late summer) was reflected in the predominant occurrence in the 0–30 m interval in the Barents Sea ecosystem cruise (Eriksen et al., 2009). Then, when approaching the drift end point (i.e., day observed in the fall), each individual's "success" was evaluated as a function of: (1) proximity to polar cod 0-group observations; (2) count of 0-group in the sample; and (3) similarity between modelled individual size and 0-group

observation sampled mean size.

2.4. OSCAR oil dispersal and fate model

The OSCAR model is a Lagrangian particle-based oil spill and fate model dividing oil into 25 pseudo-components including both droplets and dissolved oil (Carroll et al., 2018; Nordam et al., 2019). Based on the oil spill scenarios (see below) oil is introduced at six different locations with a given spill rate, duration and oil type whereby oil is weathered accounting for dispersal, entrainment into the water column, stranding, evaporation, biodegradation and emulsifications. Oil spreads horizontally and vertically due to ocean currents, turbulent mixing and droplet buoyancy according to parametrizations based on experimental work both in laboratory and field experiments as well as properties for different types of oil (Reed et al., 1999). For this study, OSCAR (version 14.2) released Wisting type oil (Singsaas et al., 2020) at 6 locations (see Fig. 2) with the southernmost spill site at the actual Wisting location (24.3E, 73.4 N) and the other 5 locations to the north in areas currently not opened to oil exploration. For each location, oil releases were initiated at the sea surface the first day of each month (January through April), for a spill duration of 28 days with a continuous constant oil release rate of 8 000 m^3/day and simulated tracking of oil dispersal for a total of 50 days. The 2021 Barents-2.5 km model archive provided forcing to OSCAR for daily model output on oil dispersal and fate supporting offline exposure analysis of polar cod ELS.

2.5. Offline coupling of data-driven model results to address main objectives

On average, about 1 million particles initiated each year fulfil the criteria of having the entire egg stage covered by ice. Subsequently, we select on average a subset of about 10 % of these particles according to their score on how well they match the 0-group observations for further analysis. As Copeman et al. (2017) shows, feeding opportunities during fall are a necessary condition for winter survival. We therefore distinguish age-0 polar cod experiencing 50 % better ambient observed fall *C. glacialis* concentrations. The *C. glacialis* data are based on average spatially observed distribution of total *Calanus* spp. biomass from vertical tows collected at the annual ecosystem cruises during August-September and the temperature-dependent *C. glacialis* fraction from the species-specific counts in the Vardø-North section (Gerland et al., 2023). We emphasize combined modelled results for 2019 polar cod ELS dispersal with the 2021 oil spill scenarios because this year represents the highest overlap with oil in all years modelled (2013–2020). However, we also present results for all years 2013–2020 to provide an understanding of inter-annual variability.

3. Results

3.1. Lagrangian coherent structures

Monthly mean FTLE based on the Barents-2.5 km modelled hourly currents for 2021 show that LCSs are much more pronounced during winter than summer, and that they follow topographic features similarly to the PF (Fig. 1). In the month of February, we see a strong repelling signal especially along the shelf edge in the western Barents Sea, and along the southern Svalbard slope. Towards the Hopen Trench the LHC bifurcates into separate structures with one closely aligned along the 200 m isobath and another weakening towards the northeast where the 300 m and 400 m isobaths diverge. In summer, here shown for the month of July, the LCSs are mostly weak, with some strong features appearing only close to land and again along the shelf edge in the

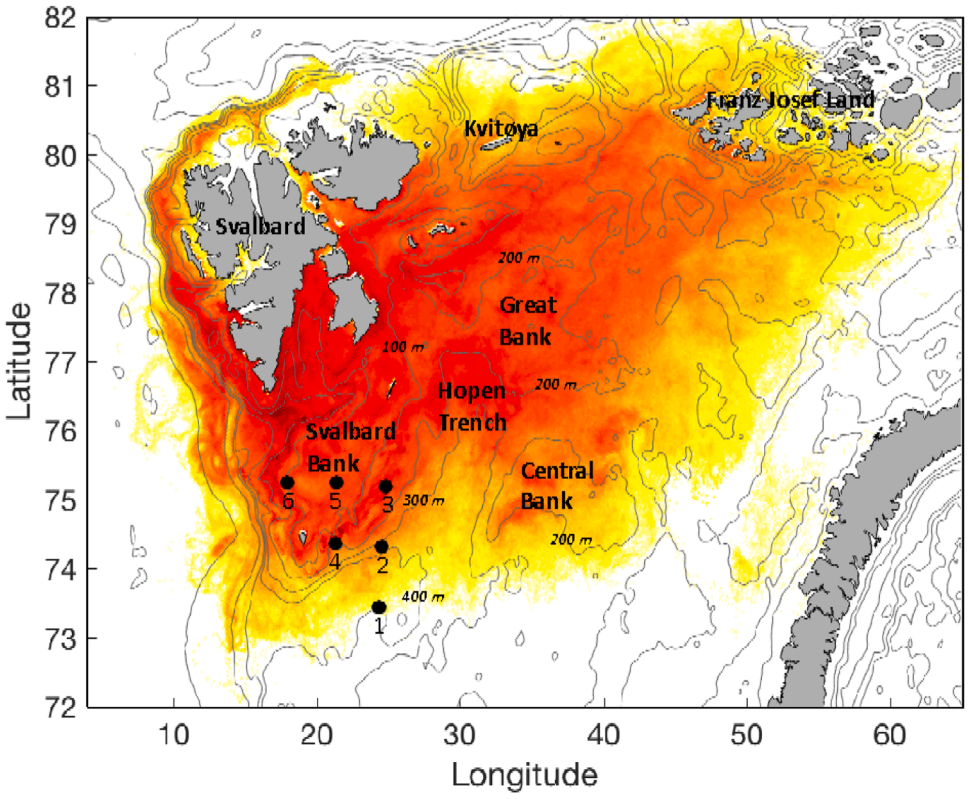

Fig. 2. All areas visited by polar cod early life stages during the dispersal from spawning until fall in 2019. Colours indicate the number of particles that visit each 4 × 4 km grid cell per day (each particle may be counted multiple times in a grid cell if staying more than one day) on a logarithmic scale ranging from white (0) to dark red (5.52). Also included are the 6 different oil spill locations identified by numbers from 1 (corresponding to the licensed oil and gas exploration site Wisting) to 6 on the western flank of the Svalbard Bank. The distance between each spill site is 100 km in the *x*- and *y*-direction. Also included are the topography (isobaths 200, 500, 1000, 2000 m) with names of locations described in the text.

western Barents Sea. The seasonal variability is distinct, with winter signals almost 3 times stronger than during summer in the section across the southern slope of the Svalbard Bank between oil spill location 1 and 5. Note, however, that there is a significant inter-monthly variability in the LCS strength.

3.2. Polar cod early life stage dispersal and exposure to oil

Polar cod ELS dispersal for the subset of individuals matching 0-group observations in 2019 occupies an area limited by the western shelf of Svalbard, the northern shelf between Svalbard and Franz Josef Land, in proximity of the PF to the south delineating the southern slope of the Svalbard Bank, the Hopen Trench and the northern slopes of the Central Bank (Fig. 2). The eastern limitation is more indefinite. Early

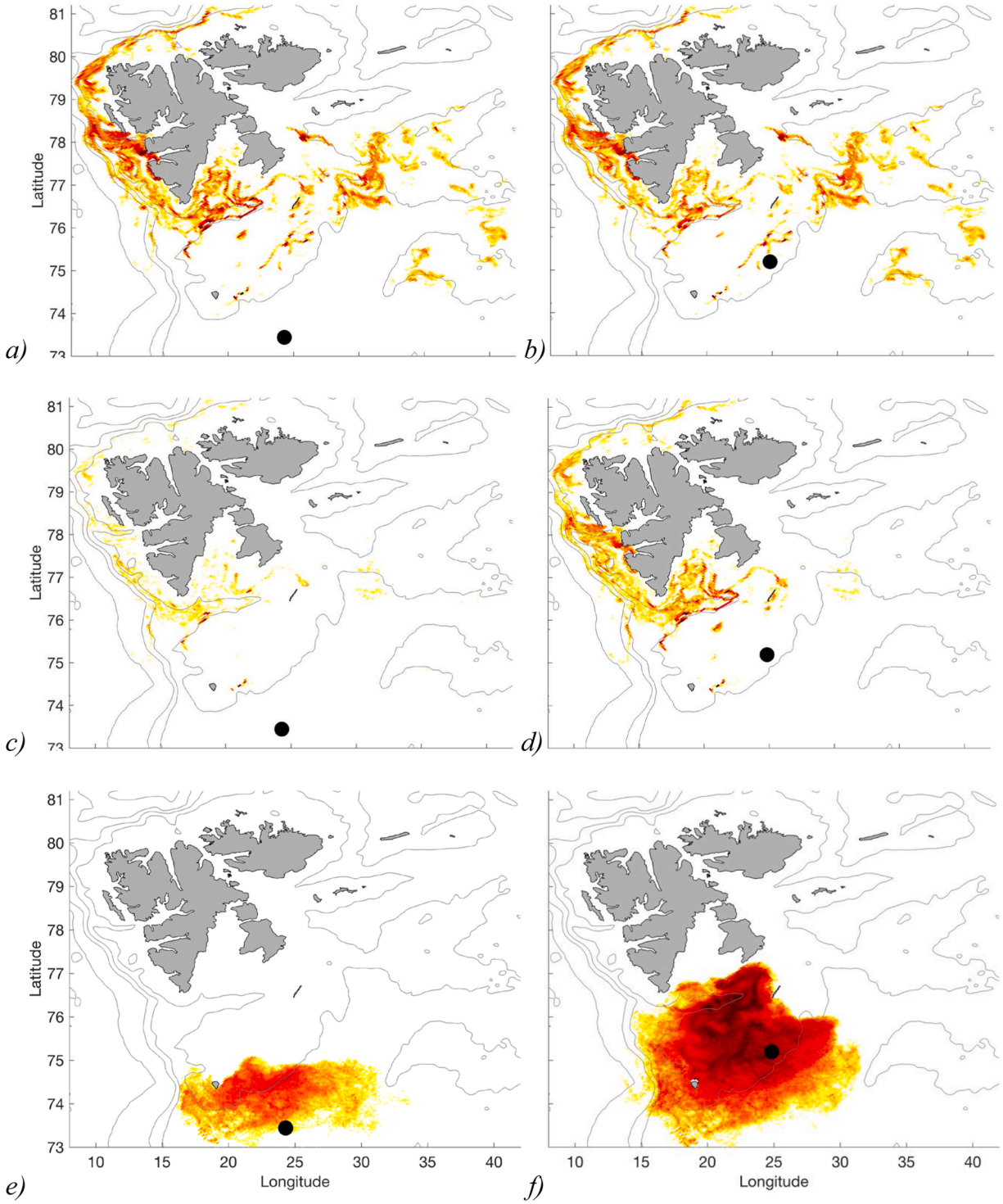

Fig. 3. Colours indicate the number of particles per 4 × 4 km grid cell on a logarithmic scale ranging from white (0) to dark red (3.3). Panels a and b: End positions for non-exposed individuals. Panels c and d: End positions for individuals exposed to oil initiated at location 1 and 3 respectively. Panels e and f: All positions where individuals have been exposed to oil during the dispersal from spawning to nursery grounds. Black dots indicate oil spill locations 1 and 3.

spawning results in dispersal trajectories farther to the northeast whereas late spawning extends ELS distributions farther to the southwest (Fig. SI1). For polar cod ELS that were not exposed to oil, fall distribution of individuals matching 0-group observations were located in areas to the south and southeast of Svalbard and along the western Svalbard shelf (Fig. 3a and b). In contrast, individuals that were exposed to oil from a spill initiated April 1st at the position of Wisting (spill location 1) were more restricted to just the southeast of Svalbard (Fig. 3c). Clearly, the part of the polar cod ELS dispersal trajectories involving exposure to oil takes place at the southern flank and slope of the Svalbard Bank across the PF (Fig. 3e). Oil spills initiated 200 km farther north (spill location 3) results in a significant increase in the number of individuals that are exposed to oil and a broader geographic range of exposure to the north, and across the entire Svalbard Bank and all the way to the southern tip of Svalbard (Fig. 3d and f).

3.3. *Intra- and inter-annual differences in polar cod early life stages exposure to oil when accounting for fall prey conditions*

Exposure of polar cod ELS to oil is sensitive to both the seasonal timing of oil spill initiation and annual variability in environmental conditions affecting dispersal (Fig. 4). The fraction of polar cod ELS exposed to oil increases with increasing day of the year for the oil spill initiation (Fig. 4a). For the northernmost spill site, the ELS fraction exposed to oil increases from about 5 to 38 % if the oil spill starts April 1st instead of January 1st, although this increase was much less distinct at the location of Wisting (oil spill location 1). The fraction of exposed polar cod ELS drops significantly if fall feeding requirements are also considered as a necessary component of 1st year survival (described above with *C. glacialis*). For the northernmost oil spill, initiated April 1st, this additional requirement decreases the fraction of polar cod ELS exposed to oil from about 38 to 13 % (Fig. 4a, solid versus broken lines).

The years 2014 and in particular 2019 have the highest fractions of polar cod ELS exposed to oil from the oil spill scenarios investigated here. For all years except 2017 the fraction of exposed polar cod ELS that also match the highest concentrations of *C. glacialis* during fall are less than half the fraction exposed to oil. The fraction of polar cod ELS exposed to oil released at Wisting (oil spill location 1) is less than 5 % for all years except for 2019, when it reaches about 7 %.

The modelled dispersal trajectories of polar cod ELS in 2019 that both matched 0-group observations and were not exposed to oil originated from a wide range of spawning dates from December 1st until April 1st (Fig. 5, green columns). In contrast, the oil-exposed individuals originate mostly from mid to late spawning dates (Fig. 5, blue columns), while the ones exposed to both oil and encounter high *C. glacialis* concentrations in late fall originate from the mid spawning dates (Fig. 5, red columns).

In the scenario year resulting in the highest overall oil exposure (2019), 37 % of individuals experienced oil concentrations above the 10 μg/L threshold from an oil spill initiated at the northernmost site (3) on April 1st (Fig. 6). A similar result is found for oil spill location 2 in that same year, while a significantly lower fraction—about 11 % - experiences this for the southernmost oil spill location (1). If also requiring elevated prey availability during the fall, the fractions of individuals experiencing above 10 μg/L oil as compared to any oil concentration do not appreciably change, except for 2014 when fall prey requirements were essentially not met. In the 2019 example year, the fraction of individuals experiencing above 10 μg/L as compared to any oil concentration is either increasing (oil spill location 1 and 2) or remaining close to constant (oil spill location 3) through the season, both with and without the additional criteria of elevated fall prey availability.

4. Discussion

Combining models for ocean dynamics, oil spill and fate, and polar cod ELS with selected oil spill scenarios reveal that sea ice and the PF limit horizontal exchange of pollutants and plankton in the northwestern Barents Sea. These natural barriers act primarily early in the year and lessen towards summer as sea ice seasonally retreat and the PF weakens. The winter-time PF structure, as revealed by the modelled FTLE here, closely resembles the features described in Oziel et al., (2016) based on in situ observations aboard research cruises during fall, with a separation into a northern and southern PF of increasing distance towards the east. Similarly, Fer and Drinkwater (2014) surveyed across the Hopen Trench and onto the Svalbard Bank in May 2008 and revealed a double front defined by salinity and temperature gradients in the south and tidal features in the north. Hence, the spatial positioning and time of oil pollution events have great significance for the exposure and survival trajectories of polar cod ELS. While the main spawning ground in the northwestern BS is to the east of Svalbard, the exposure of individuals to oil spill scenarios investigated here takes place south of Svalbard as larvae drift across the Svalbard Bank. Hence, early in the year, with an extensive ice cover, eggs are initially sheltered from oil spills occurring to the south, but exposed as larvae as the year class drifts towards the western BS in ice free waters. This is significantly more pronounced if the spill takes place in spring than during winter given that spawning

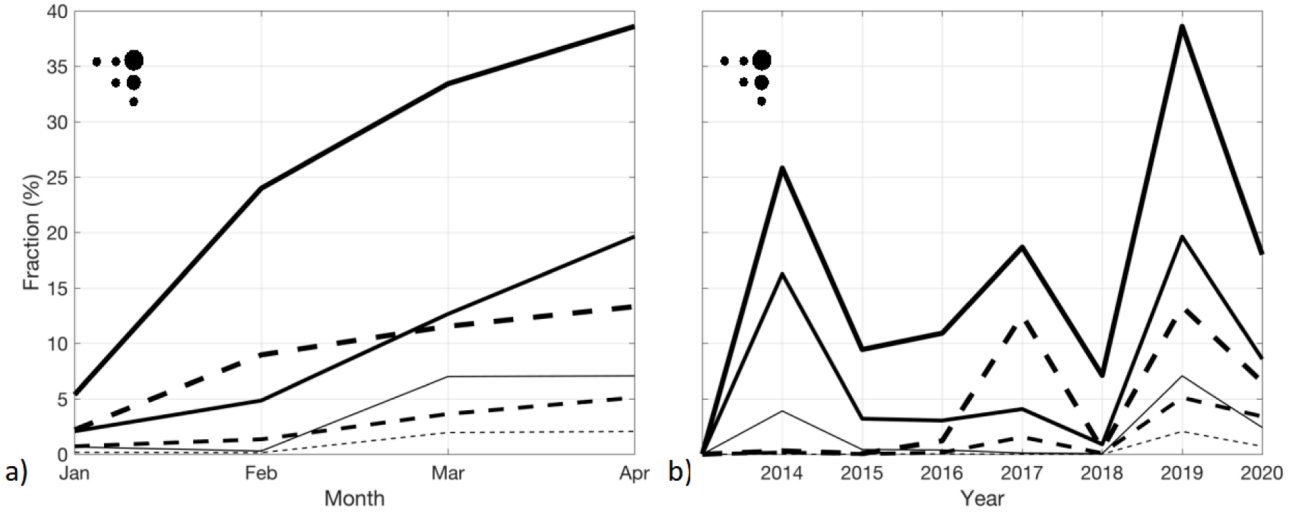

Fig. 4. Fraction of polar cod offspring distribution in 2019 exposed to oil (solid) while also facing high fall prey abundance (broken) as a function of oil spill initiation month (a) or year of polar cod offspring dispersal when oil spill is initiated April 1st (b).

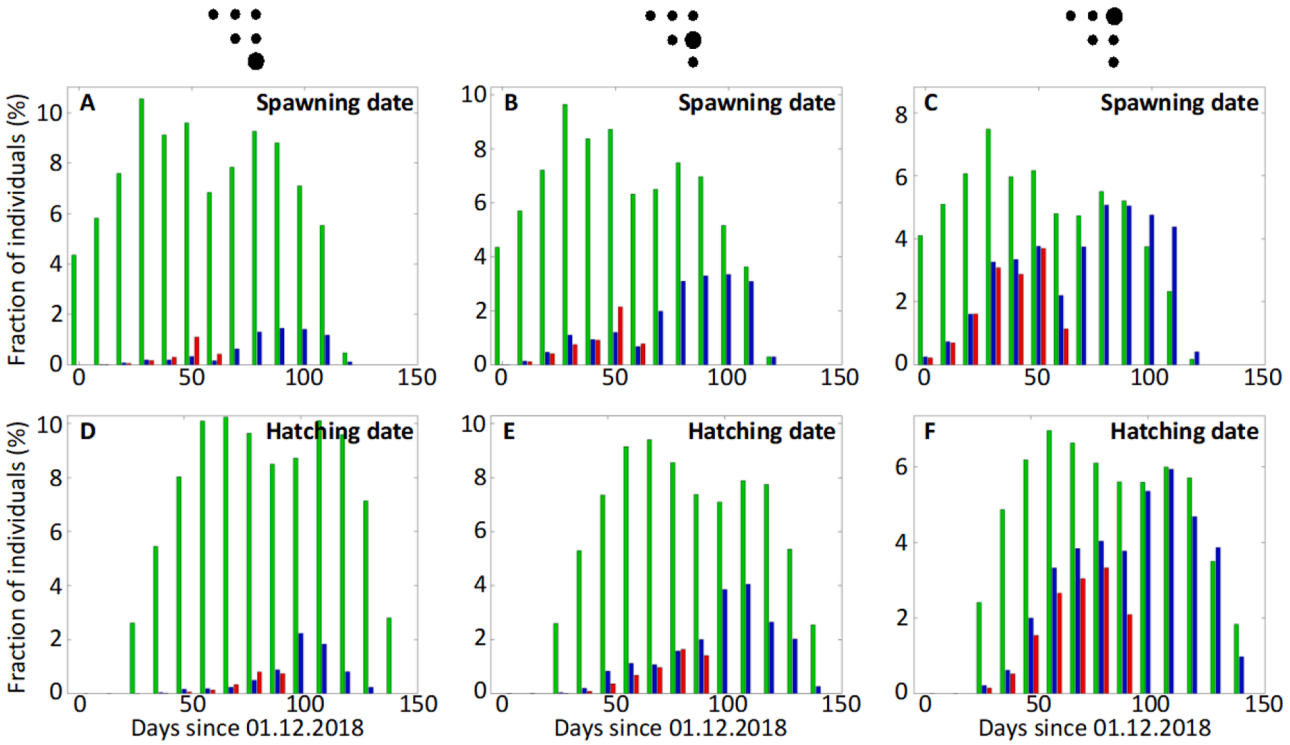

Fig. 5. Spawning dates (a, b and c) for individuals not exposed to oil (green), exposed to oil (blue) or exposed to oil and well fed during fall (red) for different oil spill sites and oil spill releases April 1st. Similar panels are shown for hatching dates (d, e and f).

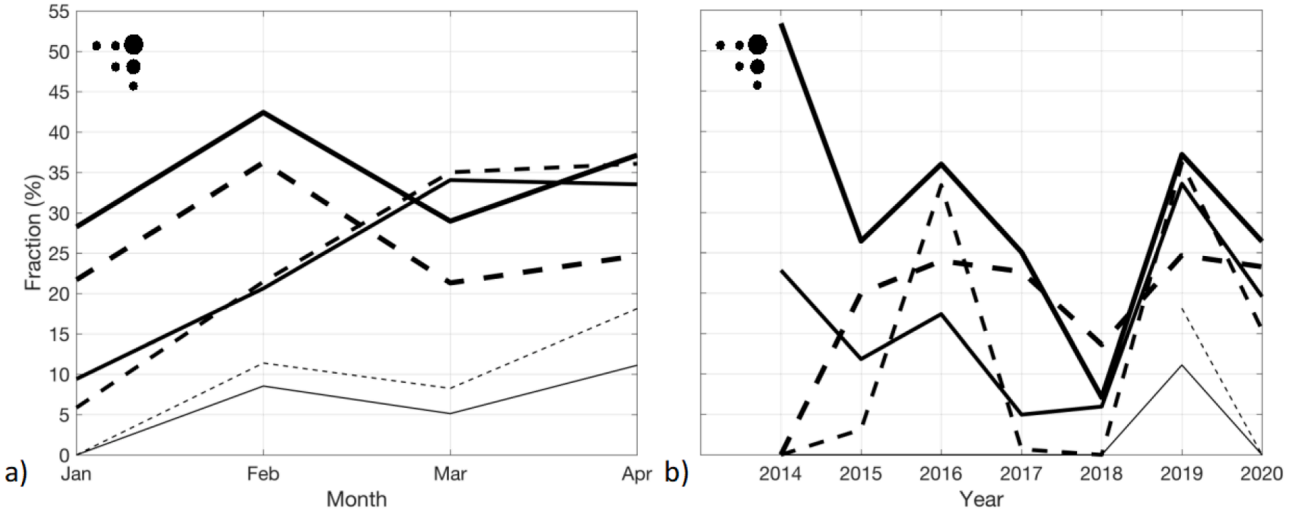

Fig. 6. Fraction of polar cod offspring distribution in 2019 exposed to oil above 10 μg/L vs. any concentrations (solid) while also encountering sufficient fall prey abundance (broken) as a function of oil spill initiation month (a) or year of polar cod offspring dispersal when oil spill is initiated April 1st (b).

occurs from December through March. The combined models indicate that seasonal shifts in dispersal trajectories of polar cod ELS are to the northeast for early spawned individuals as opposed to southwest for late spawned individuals, and this contributes to the amplified exposure of ELS for oil spills later in the year. In general, the farther north the spill occurs, the higher the fraction of polar cod ELS are affected by way of greater penetration of oil into polar cod ELS habitat.

4.1. Oil spill exposure and polar cod ELS with elevated probability of surviving through winter

As described in Copeman et al. (2017), polar cod ELS survival through the first winter depends on lipid reserves gained through foraging on lipid-rich *C. glacialis* in the fall. While there are multiple ways to assess whether such prey conditions are satisfied, both by extensive in situ sampling or ecosystem modelling, each method comes with a high degree of uncertainty. For example, field observations of early fall zooplankton aboard the annual Barents Sea Ecosystem Cruise are not recorded as stage specific occurrences (Eriksen et al., 2020). On the other hand, ecosystem models resolving zooplankton species composition and stage distribution do not fully account for zooplankton predation by numerous competing species (Aarflot et al., 2023). The prey estimates used in our study attempt to resolve some of these uncertainties by combining species and stage-specific observed

zooplankton abundance from the Vardø Nord section (that intersects the core of the polar cod ELS habitat) with species-specific observed zooplankton abundances from the Barents Sea Ecosystem Cruise. This approach accounts for some degree of predation as these numbers represent the remaining *C. glacialis* during early to mid fall available for polar cod ELS building of lipid reserves before winter. The combined observation data show that elevated abundances in *C. glacialis* occur mainly in the northern central BS and do not support polar cod ELS drifting south of Svalbard across the Svalbard Bank where there is higher likelihood of oil exposure in the scenarios investigated in this study. Hence, the results presented here indicate that natural mortality through starvation may dampen the impact of the oil spill scenarios assessed here because a significant number of individuals exposed to oil also face fall feeding conditions unfavorable to winter survival.

4.2. Exposure concentrations and fractions of polar cod ELS involved

The fraction of polar cod ELS exposed to oil under the oil spill scenarios investigated here reached a maximum of about 38 % of a year class for the northernmost spill site initiated on the latest scenario date of April 1st. Oil toxicity thresholds for ELSs of cold water marine species are complex and largely depend on how, when and whether sublethal effects (e.g. malformation, behavioural changes) contribute to delayed mortality beyond acute mortality measures under experimental conditions (e.g., Sørhus et al., 2023; Cresci et al., 2020). Laurel et al. (2019) concluded that their low treatment of polar cod with 3 days of embryonic exposure to 0.65–1.1 μg/L TPAH led to dysregulation of lipid metabolism and growth into the late summer juvenile period despite no morphological changes near the time of oil exposure. Hence, low levels of exposure to oil reduces growth and lipid content at a critical time when larvae and juveniles need to acquire energy to survive food-limited winter conditions. In our oil spill scenarios, we see that less than half the individuals exposed to oil by the northernmost oil spill experienced exposure levels above 10 μg/L. The exposed fraction increases with latitude for the oil spill with little seasonal variation. Still, for the northernmost oil spill initiated April 1st, about 38 % of the year class is exposed to oil while about 14 % of the year class is exposed above 10 μg/L oil.

4.3. Climate change impact on oil spill effects to polar cod early life stages

Both sea ice and the PF seem to act as natural barriers for surface (especially in winter) and near-surface oil dispersal into the habitat of polar cod ELS if oil is released farther south. Furthermore, ice shelters polar cod eggs from mechanical stress caused by breaking waves and retain them underneath the ice during ice drift. However, dispersal trajectories for polar cod diverge from ice movements as eggs hatch and larvae occupy the upper water column. While the sea ice extent in the Barents Sea is temporally dynamic with a general climate change induced retreat (Årthun et al., 2012), the position of the PF remains steady with modest variation in the strength of its temperature and salinity gradients. However, as reported previously by Lind et al. (2014), there are ongoing changes in the 3D distribution of the water mass at the intersection between AW and PW in the northern Barents Sea. At this intersection, the bottom edge of the PW is eroded by the AW due to both the increased inflow of heat from the south and reduced sea ice import from the north. In total, this weakens the conditions for maintaining the topographic-controlled PF separating AW and PW where it is today. These changes will likely lead to a warmer, well-mixed northern Barents Sea resembling an Atlantic climate regime (Lind et al., 2014). If AW displaces PW northwards, there will still be topographic steering of plankton and pollutant exchange across the region holding the PF, but this will likely be weakened as temperature and salinity gradients are eroded away and topographic frontal structures are unable to limit transport between AW and PW. How rapid such a transition may occur depends on greenhouse gas emissions and the response to that in the earth system. Chylek et al. (2024) show that among 19 CMIP6 models the range of Arctic surface air temperature in 2100 given a SSP2-4.5 "middle of the road" scenario spans from 4 to 9 °C. Therefore, climate change is likely to dramatically change the environmental conditions in the northern Barents Sea, thereby outdating any risk assessment of anthropogenic impacts on key Arctic species that do not consider such changes. Climate change essentially amplifies uncertainties in temporal risk assessment in this region. Furthermore, if sea ice retreat continues at the current rate the northwestern Barents Sea spawning grounds of polar cod are likely to be marginalized towards the Arctic continental shelf edge and effectively more vulnerable to all anthropogenic pressures.

4.4. Recommendations for future experimental, in situ and modelling work

Natural mortality schedules remain poorly understood for polar cod, making it difficult to quantify the absolute impacts of anthropogenic stressors such as oil spills. Therefore, seasonal observations in the condition and abundance of larvae and juvenile (e.g., "follow the cohort approach") alongside ecosystem monitoring will be necessary to contextualize novel sources of mortality that may occur earlier in the year (e.g., spring oil spills) from variation in natural mortality occurring later in the year, e.g. winter stress. We recommend periodic ecosystem monitoring on seasonal scales to complement the existing annual survey. This includes tracking the zooplankton assemblage alongside lipid content of polar cod from fall to winter to spring. While previous studies have shown the importance of *C. glacialis* to polar cod, establishing links to these prey sources (e.g. stomach analyses, fatty acid biomarkers) and their impacts on the energetic status of ELS are necessary. This includes the relative role of *C. glacialis* vs. opportunistic feeding on *C. finmarchicus*, an alternative prey item in parts of the polar cod habitat. Polar cod also need to contend with capelin (*Mallotus villosus*) following the retreating sea ice in the northern Barents Sea, which may compete with polar cod for common prey items (Dalpadado et al., 2024). Both represent key prey species for fish and mammals. Understanding these trophic connections through combined observations and modelling will be necessary to both determine their ecosystem service and evaluate anthropogenic impacts on their abundance. Collecting such data is particularly difficult beneath ice (Ingvaldsen et al., 2023), but new technologies and approaches are making it possible (Schaafsma et al., 2024). On finer scales we also see a specific need for data on vertical behavioural of larval polar cod, size-specific growth and lipid metabolism under natural environments and following exposure to oil. This would lead to improved understanding of processes determining growth and energy potential that could be incorporated into model formulations in support of assessing risks of human activities in or close to Arctic ecosystems.

4.5. Inconsistency in model forcing

The current modelling study has used two different ROMS model archives as input to the oil spill and fate model, and the polar cod IBM, respectively. The oil spill and fate scenario modelling with the 6 different but comparable scenarios have used a ROMS simulation with a 2.5 × 2.5 km horizontally resolved grid covering 2021 (Röhrs et al., 2023). At the time when this work was carried out, the ocean model archive was restricted to a single year of simulations due to available computational resources. In contrast, the coarser resolution of the polar cod ELS IBM (ROMS 4 × 4 km horizontally resolved grid) allowed for multiple years to be used for this study (Lien et al., 2014). Lack of consistency between temporal coverage in the physical forcing of the two model components—oil spill and fate vs IBM—is expected to be more important than the modest difference in spatial resolution. However, results presented here should be interpreted with care as interannual environmental variability in the physical forcing is to be expected and will influence quantification of oil spill exposure of polar cod ELS. In

the continuation of this work, we will use the planned Barents-2.5 km Ensemble Prediction System (EPS) recently established by MET Norway to provide more realistic exposure estimates and ensemble members for uncertainty simulation of oil spill and ELS dispersal.

5. Conclusion

By combining data-driven models for the ocean, oil spill and fate, and individual-based early life stages of the key Arctic species polar cod we find that the sea ice and the Polar Front in the Barents Sea act as natural barriers between pollutants in the Atlantic Water and polar cod eggs and larvae in the Polar Water. However, the barrier effect varies extensively through the season, typically weakening from winter towards summer, despite the year-round presence of the Polar Front. The seasonal exposure intensity of polar cod to oil is highly variable, suggesting petroleum regulations should be implemented with temporal and spatial limitations varying through the year. However, climate change will cause continued sea ice retreat and a likely weakening of the Polar Front and its barrier effect. The validity of any anthropogenic impact risk assessment in the vicinity of the ice edge zone and the Polar Front will therefore depend on updated oceanographic observations or climate-driven forecasts.

CRediT authorship contribution statement

Frode B. Vikebø: Writing – original draft, Visualization, Validation, Software, Resources, Project administration, Methodology, Investigation, Funding acquisition, Formal analysis, Data curation, Conceptualization. **Raymond Nepstad:** Writing – original draft, Software, Methodology, Investigation, Formal analysis, Data curation, Conceptualization. **Mateusz Matuszak:** Writing – original draft, Software, Methodology, Investigation, Formal analysis, Data curation. **Edel S.U. Rikardsen:** Writing – original draft, Software, Investigation, Data curation. **Benjamin J. Laurel:** Writing – original draft, Supervision, Methodology, Investigation, Funding acquisition, Conceptualization. **Sonnich Meier:** Writing – original draft, Supervision, Investigation, Conceptualization. **Elena Eriksen:** Writing – original draft, Supervision, Investigation, Data curation, Conceptualization. **Johannes Röhrs:** Writing – original draft, Software, Methodology, Investigation, Data curation, Conceptualization. **Kai H. Christensen:** Writing – original draft, Software, Methodology, Investigation, Data curation, Conceptualization. **Malgorzata Smieszek-Rice:** Writing – original draft, Investigation, Conceptualization. **Alf Håkon Hoel:** Writing – original draft, Investigation, Conceptualization. **Mats Huserbråten:** Writing – original draft, Validation, Supervision, Software, Methodology, Investigation, Formal analysis, Data curation, Conceptualization.

Declaration of competing interest

The authors declare that they have no known competing financial interests or personal relationships that could have appeared to influence the work reported in this paper.

Acknowledgement

The work presented was funded by the NFR project Arctic ecosystem impact assessment of oil in ice under climate change - Action (314449/E40).

Supplementary materials

Supplementary material associated with this article can be found, in the online version, at doi:10.1016/j.aquatox.2025.107293.

Data availability

Data will be made available on request.

References

Aarflot, J.M., Eriksen, E., Prokopchuk, I.P., Svensen, C., Søriede, J.E., Wold, A., Skogen, M., 2023. New insights into the Barents Sea *Calanus glacialis* population dynamics and distribution. Prog. Oceanogr. 217. https://doi.org/10.1016/j.pocean.2023.103106.

ACIA, 2005. Arctic Climate Impact Assessment. Cambridge University Press, p. 1020. ACIA Overview report.

AMSA, 2009. Arctic Marine Shipping Assessment Report. Arctic Council.

Årthun, M., Eldevik, T., Smedsrud, L.H., Skagseth, Ø., Ingvaldsen, R.B., 2012. Quantifying the influence of Atlantic heat on the Barents Sea ice variability and retreat. J. Climate 25.

Atadzhanova, O., Zimin, A., Svergun, E., Konik, A., 2018. Submesoscale eddy structures and frontal dynamics in the Barents Sea. Phys. Oceanogr. 25, 220–228. https://doi.org/10.22449/1573-160X-2018-3-220-228.

Bender, M.L., Giebichenstein, J.., Teisrud, R.N., Laurent, J., Frantzen, M., Meador, J.P., Sørensen, L., Hansen, B.H., Reinardy, H.C., Laurel, B., et al., 2021. Combined effects of crude oil exposure and warming on eggs and larvae of an arctic forage fish. Sci. Rep. 11, 8410. https://doi.org/10.1038/s41598-021-87932-2.

Bouchard, C., Mollard, S., Suzuki, K., Robert, D., Fortier, L., 2016. Contrasting the early life histories of sympatric Arctic gadids *Boreogadus saida* and *Arctogadus glacialis* in the Canadian Beaufort Sea. Polar Biol. 39, 1005–1022. https://doi.org/10.1007/s00300-014-1617-4.

Carroll, J., Vikebø, F., Howell, D., Broch, O.J., Nepstad, R., Augustine, S., Skeie, G.M., Bast, R., Juselius, J., 2018. Assessing impacts of simulated oil spills on the Northeast Arctic cod fishery. Mar. Pollut. Bull. 126, 63–73. https://doi.org/10.1016/j.marpolbul.2017.10.069.

Chylek, P., Folland, C.K., Klett, J.D., Wang, M., Lesins, G., Dubey, M.K., 2024. Why does the ensemble mean of CMIP6 models simulate arctic temperature more accurately than global temperature? Atmosphere 15 (5), 567. https://doi.org/10.3390/atmos15050567.

Copeman, L.A., Laurel, B.J., Spencer, M., Sremba, A., 2017. Temperature impacts on lipid allocation among juvenile gadid species at the Pacific Arctic-Boreal interface: an experimental laboratory approach. Mar. Ecol. Prog. Ser. 566, 183–198. https://doi.org/10.3354/meps12040.

Cresci, A., Paris, C.B., Browman, H.I., Skiftesvik, A.B., Shema, S., Bjelland, R., Sørhus, E., 2020. Effects of exposure to low concentrations of oil on the expression of cytochrome P4501a and routine swimming speed of Atlantic Haddock (*Melanogrammus aeglefinus*) larvae in situ. Environ. Sci. Technol. 54 (21), 13879–13887.

Dalpadado, P., Prokopchuk, I.P., Bogstad, B., Skaret, G., Ingvaldsen, R.B., Dolgov, A.V., Boyko, A.S., Rey, A., Ono, K., Bagøien, E., Huse, G., 2024. Zooplankton link climate to capelin and polar cod in the Barents Sea. Prog. Oceanogr.226.

Eriksen, E., Prozorkevich, D., Dingsør, G., 2009. An evaluation of 0 group abundance indices of Barents Sea fish stocks. Open Fish Sci. J. 2, 6–14.

Eriksen, E., Huserbråten, M., Gjøsæter, H., Vikebø, F., Albretsen, J., 2020. Polar cod egg and larval drift patterns in the Svalbard archipelago. Polar Biol. 43, 1029–1042.

Fer, I., Drinkwater, K., 2014. Mixing in the Barents Sea Polar Front near Hopen in spring. J. Mar. Sys. 130.

Ferguson, R.M.W., Gontikaki, E., Anderson, J.A., Witte, U., 2017. The variable influence of dispersant on degradation of oil hydrocarbons in subarctic deep-sea sediments at low temperatures (0–5 °C). Sci. Rep. 7, 2253.

Gerland, S., et al., 2023. Still Arctic?—The changing Barents Sea. Elem. Sci. Anthr. 11, 1. https://doi.org/10.1525/elementa.2022.00088.

Gjøsæter, H., Huserbråten, M.B.O., Vikebø, F., Eriksen, E., 2020. Key processes regulating the early life history of Barents Sea polar cod. Polar Biol. 43, 1015–1027. https://doi.org/10.1007/s00300-020-02656-9.

Haug, T., Bogstad, B., Chierici, M., Gjøsæter, H., Hallfredsson, E.H., et al., 2017. Future harvest of living resources in the Arctic Ocean north of the Nordic and Barents Seas: a review of possibilities and constraints. Fish. Res. 2017 (188), 38–57. https://doi.org/10.1016/j.fishres.2016.12.002.

Huserbråten, M.B.O., Eriksen, E., Gjøsæter, H., Vikebø, F., 2019. Polar cod in jeopardy under the retreating Arctic sea ice. Commun. Biol. 2 (1). https://doi.org/10.1038/s42003-019-0649-2.

Ingvaldsen, R.B., Eriksen, E., Gjøsæter, H., Engås, A., Schuppe, B.K., Assmann, K., Cannaby, H.A., Dalpadado, P., Bluhm, B., 2023. Under-ice observations by trawls and multi-frequency acoustics in the Central Arctic Ocean. Sci. Rep. 13 (1000).

Kolås, E.H., Fer, I., Baumann, T.M., 2024. The polar front in the northwestern Barents Sea: structure, variability and mixing. Ocean Sci. 20, 895–916. https://doi.org/10.5194/os-20-895-2024.

Laurel, B.J., Copeman, L.A., Spencer, M., Iseri, P., 2018. Comparative effects of temperature on rates of development and survival of eggs and yolk-sac larvae of Arctic cod (*Boreogadus saida*) and walleye pollock (*Gadus chalcogrammus*). ICES J. Mar. Sci.75 (7).2403-2412.

Laurel, B.J., Iseri, P., Spencer, M.L., Hutchinson, G., Nordtug, T., Donald, C.E., Meier, S., Allan, S.E., Boyd, D.T., Ylitalo, G.M., Cameron, J.R., French, B.L., Linbo, T.L., Scholz, N.L., Incardona, J.P., 2019. Embryonic crude oil exposure impairs growth and lipid allocation in a keystone arctic forage fish. iScience 19, 1101–1113.

Lien, V.S., Gusdal, Y., Vikebø, F.B., 2014. Along-shelf hydrographic anomalies in the Nordic Seas (1960–2011): locally generated or advective signals? Ocean. Dyn. 64, 1047–1059.

Lien, V.S., Schlichtholz, P., Skagseth, Ø., Vikebø, F.B., 2017. Wind-driven Atlantic water flow as a direct mode for reduced Barents Sea ice cover. J. Clim. 30 (2), 803–812. https://doi.org/10.1175/jcli-D-16-0025.1.

Matuszak M., Röhrs J., Isachsen P.E. and Idžanović M. (2024) Persistence and robustness of Lagrangian coherent structures, EGUsphere [preprint], https://doi.org/10.5194/egusphere-2024-1171.

Melia, N., Haines, K., Hawkins, E., 2016. Sea ice decline and 21st century trans-Arctic shipping routes. Geophys. Res. Lett. 43, 9720–9728. https://doi.org/10.1002/2016GL069315.

Nahrgang, J., Dubourg, P., Frantzen, M., Storch, D., Dahlke, F., Meador, J.P., 2016. Early life stages of an arctic key-stone species (*Boreogadus saida*) show high sensitivity to awater-soluble fraction of crude oil. Environ. Pollut. 218, 605–614. https://doi.org/10.1016/j.envpol.2016.07.044.

Nordam, T., Beegle-Krause, C.J., Skancke, J., Nepstad, R., Reed, M., 2019. Improving oil spill trajectory modelling in the Arctic. Mar. Pollut. Bull. 140, 65–74.

Nordam, T., Litzler, E., Skancke, J., Singsaas, I., Leirvik, F., Johansen, Ø., 2020. Modelling of oil thickness in the presence of an ice edge. Mar. Pollut. Bull. 156.

Oziel, L., Sirven, J., Gascard, J.C., 2016. The Barents Sea frontal zones and water masses variability (1980-2011). Ocean Sci 12.

Porter, M., Henley, S.F., Orkney, A., Bouman, H.A., Hwang, B., Dumont, E., Venables, E. J., Cottier, F., 2020. A polar surface eddy obscured by thermal stratification. Geophys. Res. Lett. 47, e2019GL086281. https://doi.org/10.1029/2019GL086281.

Reed, M., Johansen, Ø., Brandvik, P.J., Daling, P., Lewis, A., Fiocco, R., Mackay, D., Prentki, R., 1999. Oil spill modeling towards the close of the 20th century: overview of the state of the art. Spill Sci. Technol. Bull. 5 (1), 3–16.

Röhrs, J., Gusdal, Y., Rikardsen, E.S.U., Durán Moro, M., Brændshøi, J., Kristensen, N.M., Fritzner, S., Wang, K., Sperrevik, A.K., Idžanović, M., Lavergne, T., Debernard, J.B., Christensen, K.H., 2023. Barents-2.5 km v2.0: an operational data-assimilative coupled ocean and sea ice ensemble prediction model for the Barents Sea and Svalbard. Geosci. Model. Dev. 16, 5401–5426. https://doi.org/10.5194/gmd-16-5401-2023.

Schaafsma, F.L., Flores, H., David, C.L., Castellani, G., Sakinan, S., Meijboom, A., Niehoff, B., Cornils, A., Hildebrandt, N., Schmidt, K., Snoeijs-Leijonmalm, P., Ehrlich, J., Ashjian, C.J., 2024. Insights into the diet and feeding behavior of immature polar cod (*Boreogadus saida*) from the under-ice habitat of the central Arctic Ocean. J. Fish Biol. 105 (3), 907–930.

Singsaas, I., Leirvik, F., Daling, P.S., Guénette, C., Sørheim, K.R., 2020. Fate and behaviour of weathered oil drifting into sea ice, using a novel wave and current flume. Mar. Pollut. Bull. 159, 111485.

Skagseth, Ø., Eldevik, T., Årthun, M., Asbjørnsen, H., Lien, V.S., Smedsrud, L.H., 2020. Reduced efficiency of the Barents Sea cooling machine. Nat. Clim. Change 10, 661–666. https://doi.org/10.1038/s41558-020-0772-6.

Spencer, M.L., Vestfals, C.D., Mueter, F.J., Laurel, B.J., 2020. Ontogenetic changes in the buoyancy and salinity tolerance of eggs and larvae of polar cod (*Boreogadus saida*) and other gadids. Polar Biol. 43, 1141–1158.

Søreide, J.E., Leu, A., Berge, J., Graeve, M., Falk-Petersen, S., 2010. Timing of blooms, algal food quality and *Calanus glacialis* reproduction and growth in a changing Arctic. Glob. Change Biol. 16, 3154–3163.

Sørhus, E., Sørensen, L., Grøsvik, B.E., Goff, J.L., Incardona, J.P., Linbo, T.L., Baldwin, D. H., Karlsen, Ø., Nordtug, T., Hansen, B.H., Thorsen, A., Donald, C.E., van der Meeren, T., Robson, W., Rowland, S.J., Rasinger, J.D., Vikebø, F.B., Meier, S., 2023. Crude oil exposure of early life stages of Atlantic haddock suggests threshold levels for developmental toxicity as low as 0.1 µg total polyaromatic hydrocarbon (TPAH)/L. Mar. Pollut. Bull. 190.

Vestfals, C.D., Mueter, F.J., Hedstrom, K.S., Laurel, B.J., Petrik, C.M., Duffy-Anderson, J. T., Danielson, S.L., 2021. Modeling the dispersal of polar cod (*Boreogadus saida*) and saffron cod (*Eleginus gracilis*) early life stages in the Pacific Arctic using a biophysical transport model. Prog. Oceanogr. 196, 102571.

WGIBAR, 2021. Working group on the integrated assessments of the Barents Sea (WGIBAR). ICES Sci. Rep. 3 (77), 236. https://doi.org/10.17895/ices.pub.8241.